rain toward the equator (sediment focusing), enhancing accumulation rates there, and that this focusing effect displays a glacial-interglacial variation linked to periods of carbonate dissolution (40). If correct, this effect might introduce a glacial-interglacial bias into stratigraphically based accumulation rates. Indeed, barite accumulation rates in PC72 calculated by the $^{230}\text{Th}_{\text{exs}}$ normalized method (Fig. 3C) do not display coherent, systematic, and consistent variations with climate signals. Taken at face value, this would suggest that productivity in this region does not vary systematically with global climate changes. The coherent variations in stratigraphically based barite accumulation in the two equatorial Pacific sites we studied that are apart by 30° of longitude, at 140°W and 110°W (Fig. 3A), however, would then require that sediment focusing and its secular variations be remarkably uniform along the equator. More work will be required to evaluate the reasons for the excess (overproduction) inventories of $^{230}\text{Th}_{\text{exs}}$ in equatorial sediments and their temporal change. We thus assume here that sediment focusing in the equatorial Pacific is not an important factor in our barite accumulation records and that the stratigraphically based barite accumulation rates in PC72 and 8PC (Fig. 3A) are reliable proxies for late Pleistocene productivity variations in the equatorial Pacific Ocean.

REFERENCES AND NOTES

1. W. S. Broecker, *Geochim. Cosmochim. Acta* **46**, 689 (1982).
2. W. H. Berger and G. Wefer, *Limnol. Oceanogr.* **36**, 1899 (1991).
3. J. Dymond and M. Lyle, *ibid.* **30**, 699 (1985).
4. A. Neftel, H. Oeschger, J. Schwander, B. Stauffer, R. Zumbrunn, *Nature* **295**, 220 (1982).
5. J. M. Barnola, D. Raynaud, Y. S. Korotkevitch, C. Lorius, *ibid.* **329**, 408 (1987).
6. W. H. Berger, V. S. Smetacek, G. Wefer, Eds., *Ocean Productivity and Paleoproductivity—An Overview* (Wiley, New York, 1989).
7. J. W. Murray, R. T. Barber, M. R. Roman, M. P. Bacon, R. A. Feely, *Science* **266**, 58 (1994).
8. F. P. Chavez and R. T. Barber, *Deep-Sea Res.* **34**, 1229 (1987).
9. J. Dymond, E. Suess, M. Lyle, *Paleoceanography* **7**, 163 (1992).
10. J. Dymond and R. Collier, *Deep Sea Res.* in press.
11. E. D. Goldberg and G. Arrhenius, *Geochim. Cosmochim. Acta* **13**, 153 (1958).
12. G. Arrhenius, in *The Sea*, M. N. Hill, Ed. (Wiley-Interscience, New York, 1963), vol. 3, pp. 655–727.
13. K. Bostrom *et al.*, *Lithos* **6**, 159 (1973).
14. T. M. Church, in *Marine Minerals*, R. G. Burns, Ed. (Mineralogical Society of America, Washington, DC, 1979), vol. 6, pp. 175–209.
15. A. Paytan, M. Kastner, E. E. Martin, J. D. Macdougall, T. Herbert, *Nature* **366**, 445 (1993).
16. F. Dehairs, R. Chesselet, J. Jedwab, *Earth Planet. Sci. Lett.* **49**, 529 (1980).
17. J. K. B. Bishop, *Nature* **331**, 341 (1988).
18. R. E. Bernstein, R. H. Byrne, P. R. Betzer, A. M. Greco, *Geochim. Cosmochim. Acta* **56**, 3273 (1992).
19. B. Schmitz, *Paleoceanography* **2**, 63 (1987).
20. G. B. Shimmield, N. B. Price, A. A. Kahn, *Chem. Geol.* **70**, 112 (1988).
21. H. Elderfield, *Paleoceanography* **5**, 711 (1990).
22. F. Gingele and A. Dahmke, *ibid.* **9**, 151 (1994).
23. F. Dehairs, W. Baeyens, L. Goeyens, *Science* **258**, 1332 (1992).
24. AR_{BaSO_4} were calculated using sedimentation rates which were in most core tops derived from ^{14}C data (*32, 43*). These ^{14}C sedimentation rates in most cases agree well with δ^{18}O derived rates where both were determined in the same core and are consistent with values obtained by other workers (*44*). In cores for which no ^{14}C data exist sedimentation rates were determined from δ^{18}O and carbonate stratigraphy (*44*). For the TT013 cores from data in (*43, 44*), for the VNTR01 cores from (*32*) and for PLDS cores from (*45*). The dry bulk densities (DBD) for the TT013 cores are from (*43*), for the VNTR01 cores from (*46*), and for the PLDS cores from (*45*).
25. Although it would have been more appropriate to relate the AR_{BaSO_4} to new production (all primary production associated with newly available nitrogen), we have chosen to use gross primary production data for the correlation. At present in this area direct measurements of new production are scarce, and the *f* ratios (the portion of new production from total production) (*47*) are not precisely known and tend to vary considerably in space and time (*48*). With the Eppley and Peterson equation (*47*) the conversion of primary productivity (*PP*) to new production (*NP*) yields a positive association between *NP* and AR_{BaSO_4}, and a greater difference (tenfold) between glacial and interglacial signals. Existing measurements of the *f* ratio by both ^{15}N uptake and C/N flux data (*49*) suggest that a rather small fraction of the total production is exported locally in the equatorial Pacific, consistent with low calculated *f* ratios of 0.1 to 0.3, that are considerably lower than the actual NO^{3-} concentrations suggest.
26. F. P. Chavez, K. R. Buck, R. T. Barber, *Deep-Sea Res.* **37**, 1733 (1990).
27. R. T. Barber, J. W. Murray, J. J. McCarthy, *AMBIO* **23**, 62 (1994).
28. F. P. Chavez, K. R. Buck, S. K. Service, J. Newton, R. T. Barber, *Deep Sea Res.*, in press.
29. H. Snoeckx, thesis, University of Michigan, Ann Arbor (1995).
30. R. W. Murray and M. Leinen, *Geochim. Cosmochim. Acta*, in press.
31. R. F. Anderson and Y. Lao, *Ocean Science Meeting*, ASLO, San Diego, CA, 21 to 25 February, 1994), p. 71.
32. A. Mix, personal communication.
33. R. W. Murray, M. Leinen, D. W. Murray, A. C. Mix, C. W. Knowlton, *Global Biogeochem. Cycles* **9**, 667 (1995).
34. C. Charles assisted with the cross-spectral analysis of the cores. The AR_{BaSO_4} lead is observed primarily at the 41,000-year frequency.
35. W. H. Berger, J. C. Herguera, C. B. Lang, R. Schneider, in *Carbon Cycling in the Glacial Ocean*, R. Zahn, T. F. Pedersen, M. A. Kaminski, L. Labeyrie, Eds. (Springer-Verlag, Berlin, 1994), pp. 385–412.
36. T. F. Pedersen, *Geology* **11**, 16 (1983).
37. D. K. Rea, N. G. Pisias, T. Newberry, *Paleoceanography* **6**, 227 (1991).
38. R. F. Anderson, personal communication.
39. F. Marcantonio *et al.*, *Earth Planet. Sci. Lett.* **133**, 549 (1995).
40. F. Marcantonio *et al.*, *Nature*, in press.
41. D. J. Demaster and R. H. Pope, *Ocean Science Meeting*, ASLO, San Diego, CA, 12 to 16 February 1996, p. 187.
42. J. W. Murray, M. Leinen, A. R. Isern, *Paleoceanography* **8**, 651 (1993).
43. W. H. Berger and J. S. Killingley, *Mar. Geol.* **45**, 93 (1982).
44. H. Snoeckx and D. K. Rea, *ibid.* **120**, 327 (1994).
45. R. W. Eppley and B. J. Peterson, *Nature* **282**, 677, (1979).
46. T. Platt and W. G. Harrison, *ibid.* **318**, 55 (1985).
47. J. W. Murray, J. N. Downs, S. Strom, C. L. Wei, H. W. Jannasch, *Deep Sea Res.* **36**, 1471 (1989).
48. C. W. Knowlton and M. Leinen, *International Conference on Paleoceanography*, Halifax, Canada, 10 to 14 October 1995, p. 136.
49. We thank A. C. Mix and R. F. Anderson for sharing their data with us and P. Johnson for assistance in the laboratory. Comments from W. H. Berger and J. Dymond and reviews by P. Froelich and an anonymous reviewer improved this manuscript. This work was supported by funds from the National Science Foundation OCE#91-16010 and the American Chemical Society PRF#27886AC8. Sediment samples were provided by the OSU core repository supported by NSF grant OCE-9102881 and the URI core repository supported by NSF grant OCE-9102410.

7 May 1996; accepted 22 October 1996

Stability of Perovskite ($MgSiO_3$) in the Earth's Mantle

Surendra K. Saxena, Leonid S. Dubrovinsky, Peter Lazor,
Yngve Cerenius, Patrik Häggkvist, Michael Hanfland,
Jingzhu Hu

Available thermodynamic data and seismic models favor perovskite ($MgSiO_3$) as the stable phase in the mantle. $MgSiO_3$ was heated at temperatures from 1900 to 3200 kelvin with a Nd-YAG laser in diamond-anvil cells to study the phase relations at pressures from 45 to 100 gigapascals. The quenched products were studied with synchrotron x-ray radiation. The results show that $MgSiO_3$ broke down to a mixture of MgO (periclase) and SiO_2 (stishovite or an unquenchable polymorph) at pressures from 58 to 85 gigapascals. These results imply that perovskite may not be stable in the lower mantle and that it might be necessary to reconsider the compositional and density models of the mantle.

The Earth's lower mantle has been thought to consist of principally the iron-magnesium silicate perovskite with an average composition of 10 to 15 mole percent of the iron component and some magnesiowustite (*1*, *2*). Ito *et al.* (*3*) showed experimentally that

Table 1. Description of the samples. All samples contained ruby. Sample 1 was kept under pressure after laser heating and was studied in situ; ruby at the edge and platinum at the center were used as pressure standards (see Fig. 1). Temperature is for the metal foil and the range includes 3 to 5% estimated error. Natural enstatite (almost pure $MgSiO_3$ with less than 1% aluminum and iron) obtained from U. Hålenius (Stakholmen, Hälsingland, Sweden, Riiksmuseet, Stockholm) was used in samples 1 and 7. The other enstatite (pure $MgSiO_3$) was synthesized from melt by H. Skogby. Perovskite (pure $MgSiO_3$) was synthesized by Y. Wang. Pt, platinum; Fe, iron; En, enstatite; Fo, forsterite; Pv, perovskite; St, stishovite; and S, silica phase (Fig. 2A).

N	Comp.	*P* (GPa)	*T* (K)	Prod.
1	Pt+En	62–86	1900–2300	MgO,S
2	Pt+En	70–100.2	2600–2900	MgO,St
3	Fe+Pv	57.5–70.0	2200–2600	MgO,St
4	Fe+En	45.4–63.8	2500–3200	Pv
5	Fe+En	70.0–90.0	2600–3000	MgO,St
6	Fe+Fo	80–100.0	2600–3000	MgO,St
7	Pt+En	35–48	1900–2600	Pv

iron containing perovskite, when heated to 1373 K or more at a pressure of ~24 GPa, forms a mixture of a low-iron perovskite (Mg,Fe)SiO_3, magnesiowustite, and stishovite. In a recent study, Meade *et al.*(*4*) noted a similar reaction when a perovskite ($Mg_{.864}$,$Fe_{.136}$)SiO_3, was heated at some unknown high temperature at 70 GPa.

Pure $MgSiO_3$ has always been assumed to be stable at mantle conditions. Its stability has been measured experimentally to pressures of about 32 GPa. To examine the stability of pure $MgSiO_3$ at higher pressures, we conducted several laser heating experiments on perovskites or enstatites and characterized the products either at the Brookhaven National Laboratory (NSLS) or at the European Synchrotron Facility (ESRF).

We conducted seven different laser-heating experiments (Table 1). The x-ray study of the quenched sample (under pressure or at 1 atm) indicates that in these laser-heating diamond-anvil cell experiments, every sample of enstatite was completely converted to perovskite. In some of the experiments at various temperatures and pressures this perovskite dissociated to periclase and SiO_2 (stishovite or maybe to one of its polymorphs). We obtained the same result when we used either perovskite or forsterite as the starting material. No actual reversals in the experiments were attempted because of experimental difficulties.

We used either platinum or iron as heating medium (Table 1) for the absorption of Nd-YAG laser. The silicate was heated indirectly by the heat from the hot metal (*5*) by scanning the sample with a 20-μm laser beam for 10 to 15 min. Pressure was measured by ruby fluorescence. The error in pressure measurement was 5% below 100 GPa and the error in temperature measurement was 3 to 5%. The cells containing iron as the laser absorber were carefully dried under vacuum for several hours to avoid any reaction with perovskite. There was no visible reaction between the metal and silicate either at the beginning or at the end of the experiments. Vacuum drying the sample prevented the iron from reacting with the silicate (*6*). If significant oxygen is present, the reaction is quite vigorous and is easily detected during heating. We scanned areas of 50 to 150 μm with x-ray beams with a size of 10 by 10 μm at ESRF and 12 by 14 μm at NSLS (*7*).

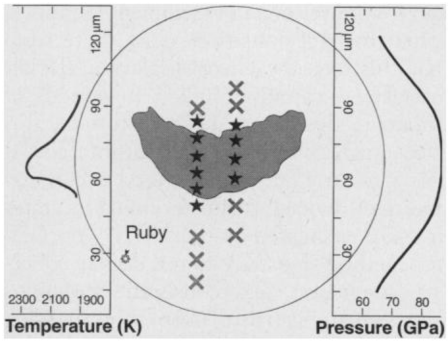

Fig. 1. Diagram of the laser-heated sample and the pressure and temperature distribution. A thin foil of platinum was sandwiched between the enstatite ($MgSiO_3$) crystals in a 120-μm size hole in a 250-μm-thick rhenium gasket. We used the Mao-Bell type diamond-anvil cell with a diamond culet size of 400 μm. A small ruby crystal was placed on one side of the gasket. The whole metal foil was scanned with a laser; for 10 to 15 min of heating. The sample was x-rayed with a beam of 14 μm in diameter. The temperature indicated is the temperature of the platinum foil measured by spectroradiometry (8). The silicate temperature will vary from this to a lower value both radially and axially. The stars represent the dissociation products MgO and SiO_2 and the crosses represent perovskite.

The results from one of the samples are shown in Fig. 1 as an example. The sample contained a small piece of platinum foil embedded in enstatite powder (Fig. 1). A rhenium gasket with a thickness of 250 μm was drilled to create a hole of 200 μm. A small ruby chip was placed on the side of the gasket hole away from the platinum foil. As we increased the pressure to about 62 GPa at the edge of the hole, the size of the hole decreased to about 120 μm. The platinum was heated to temperatures from 1900 to 2300 K by scanning a laser with a beam size of 20 μm across it for 10 to 15 min on each spot. We used the narrow slit method of spectroradiometry as described in (*8*) to determine temperature. While still under pressure, the sample was taken to NSLS for x-ray study. Because ruby was placed at the edge of the gasket hole, we used the platinum cell constants to determine the pressure of the sample. The pressure was 86 GPa at the center of the sample. Throughout the heated area over and around the platinum, all the perovskite dissociated to MgO and SiO_2 (Fig. 2A). Perovskite remained stable in the unheated or slightly heated areas. In a second sample (2, Table 1), we used a thicker platinum foil and heated several spots to temperatures between 2600 and 2900 K; enstatite was used as the starting material, and it converted to perovskite even in areas not directly heated by the laser. In such parts of the sample, the temperature could not have reached much more than 1500 K. Perovskite had dissociated to periclase and SiO_2 not only in the directly heated areas (Fig. 2B, top curve), but also away from the directly heated areas, indicating that the reaction might occur at temperatures as low as 1500 K.

In two samples, heated at pressures from 38 to 63 GPa, perovskite did not dissociate. These results indicate that the reaction may take place close to 60 GPa and that the slope of the reaction in the pressure-temperature field may not be significantly dependent on temperature (Fig. 3). We reproduced this result with three other samples.

One consequence of our results on pure $MgSiO_3$ perovskite is that perovskite of any composition may not be stable in the lower mantle. This would be the case because if another cation larger in ionic size than Mg^{2+}, for example, Al^{3+} or Ca^{2+}, replaces Mg^{2+} in the crystal lattice, the molar volume will increase making the perovskite unstable with increasing pressure. Our results are consistent with those of Meade *et al.* (*4*) but also establish that even the pure $MgSiO_3$ perovskite may not be stable in the lower mantle. It is uncertain as to what extent the dissociation of perovskite may be induced by thermal stress. Even if this effect is several gigapascals, our results are in contrast with available thermodynamic data (*2*, *9*, *10*) and the common result in seismic modeling that perovskite is stable in the lower mantle. In the thermody-

---

S. K. Saxena, L. S. Dubrovinsky, P. Lazor, Y. Cerenius, P. Häggkvist, Theoretical Geochemistry, Institute of Earth Sciences, Uppsala University, S-752 36 Uppsala, Sweden.
M. Hanfland, European Synchrotron Radiation Facility, Boite Postale 220, Avenue des Martyrs, 38043 Grenoble Cedex, France.
J. Hu, Center for High Pressure Research, Geophysical Laboratory, Carnegie Institution of Washington, Washington, DC, USA.

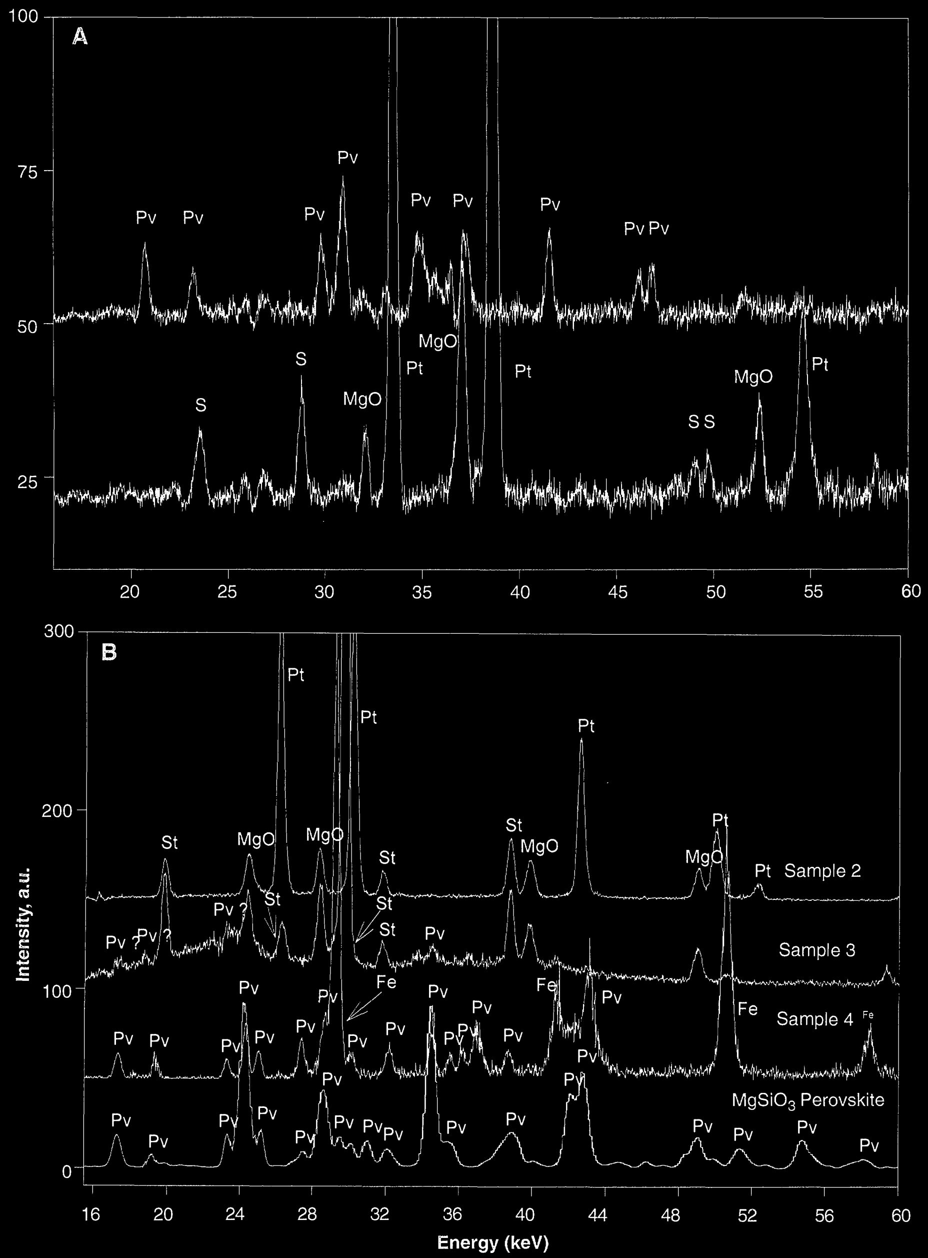

Fig. 2. X-ray data on perovskite ($MgSiO_3$) and the dissociation products. (**A**) X-ray data for the sample (1, Table 1) as pictured in Fig. 1. The top curve represents the conversion of enstatite to perovskite. The bottom curve shows the products of dissociation between pressures of 62 to 86 GPa at temperatures between 1900 to 2300 K. The reflections marked S represent a possible SiO_2 phase with structure intermediate between α-PbO_2 and ZrO_2. Two of the reflections at 3.01 A (23.63 keV) and 2.47A (28.80 keV) cannot belong to stishovite or $CaCl_2$-like silica phase (*11, 13*) but they can be easily indexed as (011) and (111) reflections of a theoretically predicted phase (*12*); $2\theta = 10.0$. (**B**) The curve at the bottom shows the x-ray diffraction of the original sample of perovskite as determined at Uppsala and used as sample 3 (Table 1). The curve labeled sample 3 is for heated perovskite. The other two curves are for samples 2 and 4 for which starting material was enstatite. The pressure and temperature of the samples are indicated in Table 1 and discussed in the text. The sample numbers are the same as in Table 1; $2\theta = 12.0$.

namic models, the extrapolation of thermal expansion to high pressure and of bulk modulus to high temperature is a significant problem (*10*). Theoretical studies (*11, 12*) indicate that a post-stishovite phase may occur at high pressures, which should have a lower volume. Using molar volume data [from (*2*) or (*10*)], we calculate that the molar volume for the new SiO_2 phase at 300 K would need to be 3% less than that of stishovite in order for the oxide mixture to become denser than perovskite at 70 GPa over a large temperature range. It is likely that the stability of a post-stishovite phase along with the effect of thermal stress may explain the dissociation of perovskite in our experiments. For mantle mineralogy, it is significant that this happens at such low pressures (relative to lower mantle) and it is thus possible that perovskite is not stable in the deep interior and is replaced by magnesiowustite and a silica phase.

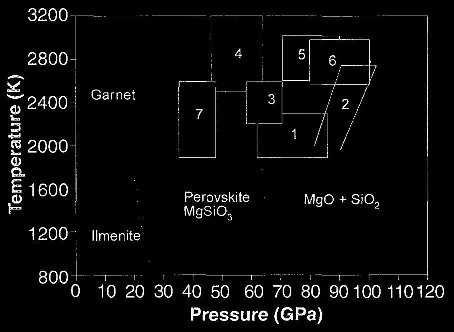

Fig. 3. The pressure-temperature phase relations for $MgSiO_3$. The sample description is given in Table 1. The temperature data reflect the maximum for the part directly in contact with the metal foil on the laser beam side.

REFERENCES AND NOTES

1. D. L. Anderson, *Theory of the Earth* (Blackwell, Boston, 1989), p. 366.
2. S. K. Saxena, *Geochim. Cosmochim. Acta* **60**, 2379 (1996).
3. E. Ito, E. Takahashi, Y. Matsui, *Earth Planet. Sci Lett.* **67**, 238 (1984).
4. C. Meade, H. K. Mao, J. Hu, *Science* **268**,1745 (1995).
5. G. Shen and P. Lazor, *J. Geophys. Res.* **100**, 17699 (1995).
6. R. Boehler, Phys. *Earth Planet. Inter.* **96**, 181 (1996).
7. The diffraction studies were carried out at the NSLS and ESRF using polychromatic synchrotron radiation. The diffraction spectra were collected with a germanium solid-state detector with 2θ angles between 10° and 12° and at energies of 5 to 80 keV.
8. P. Lazor and S. K. Saxena, in "Developments in high-pressure, high-temperature research and the study of the Earth's deep interior," *Philos. Trans. Roy. Soc.* **354**, 1307 (1966).
9. N. Funamori, T. Yagi, W. Utsumi, T. Kondo, T. Uchida, M. Seki, *J. Geophys. Res.* **101**, 8257 (1996).
10. O. Anderson, *Equations of State of Solids for Geophysics and Ceramic Science* (Oxford Univ. Press, Oxford, 1995), p. 405.
11. K. J. Kingma, R. E. Cohen, R. J. Hemley, H. K. Mao, *Nature* **374**, 243 (1995).
12. A. B. Belonoshko, L. S. Dubrovinsky, N. A. Dubrovinsky, *Am. Mineral.* **81**, 785 (1996).
13. Y. Tsuchida and T. Yagi, *Nature* **340**, 217 (1989).
14. We thank D. Hausermann for helping us with the work at the ESRF. Comments by F. Seifert and H. Annersten were helpful. We thank H. Skogby and U. Hålenius, Riiksmuseet, Stockholm, for enstatite samples.The work has been supported financially by grants from the Swedish Natural Science Research Council (NFR) and ESRF.

12 September 1996; accepted 23 October 1996